

High-capacity hydrogen storage in Al-adsorbed graphene

Z. M. Ao and F. M. Peeters*

Departement Fysica, Universiteit Antwerpen, Groenenborgerlaan 171, B-2020 Antwerpen, Belgium

(Received 22 October 2009; revised manuscript received 13 April 2010; published 5 May 2010)

A high-capacity hydrogen storage medium—Al-adsorbed graphene—is proposed based on density-functional theory calculations. We find that a graphene layer with Al adsorbed on both sides can store hydrogen up to 13.79 wt % with average adsorption energy -0.193 eV/H₂. Its hydrogen storage capacity is in excess of 6 wt %, surpassing U. S. Department of Energy (DOE's) target. Based on the binding-energy criterion and molecular-dynamics calculations, we find that hydrogen storage can be recycled at near ambient conditions. This high-capacity hydrogen storage is due to the adsorbed Al atoms that act as bridges to link the electron clouds of the H₂ molecules and the graphene layer. As a consequence, a two-layer arrangement of H₂ molecules is formed on each side of the Al-adsorbed graphene layer. The H₂ concentration in the hydrogen storage medium can be measured by the change in the conductivity of the graphene layer.

DOI: [10.1103/PhysRevB.81.205406](https://doi.org/10.1103/PhysRevB.81.205406)

PACS number(s): 68.43.-h, 81.05.U-, 84.60.Ve

I. INTRODUCTION

Recent developments in materials science have shown a rapid expansion of research toward discoveries of materials for sustainable energy. Hydrogen is being considered as an important element for future energy schemes because of its efficiency, abundance, and environmental friendliness.¹ To achieve economical feasibility, hydrogen storage materials with high gravimetric and volumetric densities, as specified by the DOE targets of 6.0 wt % mass ratio and 45 kg/m³ volumetric capacity by 2010, must be developed, and hydrogen recycling should be performed reversibly under near ambient conditions.^{1,2} Therefore, another important criteria is the binding energy per hydrogen molecule which should be within the range of -0.2 to -0.6 eV.³

Due to their light weight and high surface to volume ratio, carbon-based nanomaterials are widely studied for their applications in hydrogen storage.^{4–10} However, pristine carbon nanostructures are chemically too inert to act as a possible hydrogen storage medium.² One possible approach to increase their chemical activity is to modify the nanostructures by doping or adsorption, such as doping by alkali metals,^{6–9} transition metals,¹⁰ etc. Very recently, based on density-functional theory (DFT) calculations, Ca atoms adsorbed on graphene layers and fullerenes were found to result in high-capacity hydrogen storage mediums, which could be recycled at room temperature.^{4,5} In these systems, the adsorbed Ca atoms become positively charged and the semimetallic graphene changes into a metallic state, while the hydrogen storage capacity (HSC) can be up to 8.4 wt %. However, a recent report claimed that DFT calculations overestimated significantly the binding energy between the H₂ molecules and the Ca⁺¹ cation centers.¹¹ On the other hand, Al-doped graphene where one Al atom replaces one C atom of a graphene layer was reported as a promising hydrogen storage material at room temperature with HSC of 5.13 wt %.¹² It was found that Al alters the electronic structure of both the graphene layer and the H₂ molecules. The underlying mechanism of HSC enhancement is caused by the overlapping bands of the H₂ with those of Al and C.

In this work, we apply density-functional theory and study hydrogen adsorption on graphene with Al atoms. The

favorite adsorption configuration of Al atoms on single side and on both sides of a graphene layer are determined. The obtained materials are studied for adsorption of H₂ molecules and we discuss its hydrogen storage properties.

II. CALCULATION METHODOLOGY

Previous studies^{12–14} have shown that prediction of the physisorption energies of H₂ on the surface of graphite and carbon nanotubes as based on the local-density approximation (LDA) are in good agreement with experiments. The reliability of LDA is based on the following two facts:¹³ (1) when the electron densities of H₂ and graphene overlap weakly, the exchange-correlation energy density functional produces an attractive interaction even without any electron-density redistribution; (2) the overestimate of the binding energy by LDA (Refs. 15 and 16) is almost compensated by the neglect of the van der Waals interactions.¹³ In contrast, DFT calculations using a uniform generalized gradient approximation (GGA) usually produced purely repulsive interactions. For example, using a GGA-PW91 functional, a repulsive interaction between H₂ and a graphene layer and also between H₂ and a (6,6) carbon nanotube was found.¹⁷ This contradicts the experimental findings of Ref. 2. It is worthy to note that LDA calculations well reproduce the empirical interaction potentials between graphitic layers and also in other graphitic systems, although LDA is not able to reproduce the long-range dispersion interaction, such as van der Waals interaction.¹⁸ These facts motivated us to select the LDA for our present work. In our calculations, identical conditions are employed for the isolated H₂ molecules, the Al atom and graphene, and also for the adsorbed graphene system. The k point is set to $20 \times 20 \times 1$ for all slabs, the convergence tolerance of energy is 1.0×10^{-6} hartree (1 hartree = 27.21 eV), and that of maximum force is 1.0×10^{-4} hartree/Å.

All DFT calculations are performed using the DMOL3 code.¹⁹ Double numerical plus polarization is taken as the basis set, which has been shown to be highly accurate.¹⁹ In our simulation, three-dimensional periodic boundary conditions are applied and the H-H bond length is set to $l_{\text{H-H}}$

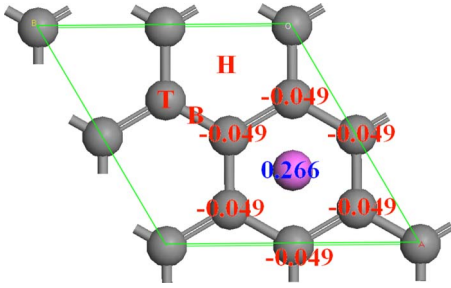


FIG. 1. (Color online) Three different sites for an Al atom adsorbed on graphene. H, B, and T denote the hollow of hexagon, bridge of C-C bond, and top site of C atom, respectively. In addition, the charges of atoms near the adsorbed Al atom are also given, where the unit of charge is one electron charge e which is not given in the figure for clarity. The gray (dark) and pink (light) balls in this figure and figures below are C and Al atoms, respectively.

$=0.74 \text{ \AA}$ identical to the experimental value.²⁰ The computational unit cell consists of a $2 \times 2 \times 1$ graphene supercell with a vacuum width of 18 \AA to minimize the interlayer interaction. As shown in Fig. 1, the supercell contains eight C atoms. All atoms are allowed to relax in all calculations.

The binding energy of Al atoms onto graphene $E_{b\text{-Al}}$ is defined as

$$E_{b\text{-Al}} = [E_{n\text{Al-graphene}} - (E_{\text{graphene}} + nE_{\text{Al}})]/n, \quad (1a)$$

where $E_{n\text{Al-graphene}}$, E_{graphene} , and E_{Al} are the energy of the system with n Al atoms adsorbed on the graphene layer, the energy of the pristine graphene layer, and the energy of one Al atom in the same slab, respectively. The binding energy of H_2 molecules onto Al-adsorbed graphene layer $E_{b\text{-H}_2}$ is defined as

$$E_{b\text{-H}_2} = [E_{i\text{H}_2+\text{Al-graphene}} - (E_{\text{Al-graphene}} + iE_{\text{H}_2})]/i \quad (1b)$$

where the subscripts $i\text{H}_2+\text{Al-graphene}$, Al-graphene , and H_2 denote the system with i H_2 molecules adsorbed, isolated Al-adsorbed graphene, and a H_2 molecule, respectively.

To investigate the potential effects of different methodologies on our results, we carried out a calculation using the cluster model with both LDA and wave-function approaches with the Møller-Plesset second-order perturbation (MP2) within the Gaussian modules where the 6-331++G* basis set was taken and maximum step size was set to 0.15 \AA . Note that the cluster configuration shown in Fig. 2 was used because of the requirement of Gaussian modules and the system was recalculated by LDA for purposes of comparison. In this calculation, a cluster with 24 carbon atoms and with one Al atom and two H_2 molecules adsorbed over the carbon surface was simulated where the dangling bonds of the C atoms at the boundary are terminated with H atoms.

III. RESULTS AND DISCUSSION

A. Adsorption of Al atoms on a graphene layer

On the basis of the published results, one may assume that the uptake capacity of hydrogen would increase if more metal atoms are adsorbed on the surface of a graphene

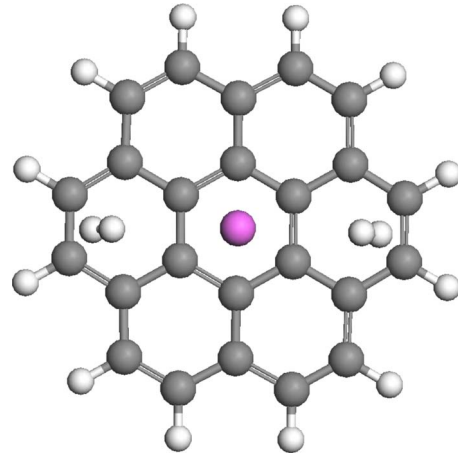


FIG. 2. (Color online) A cluster model for two H_2 molecules adsorbed on graphene with an Al atom adsorbed on its one side. The white balls are hydrogen atoms in this figure and figures below.

nanostructure.^{5,6} Furthermore, the binding between metal atoms and a surface would be strengthened if more charge is transferred between the metal atoms and the graphene nanostructure. Obviously, the binding can also be enhanced by adding more metal atoms with concomitant additional charges available for electronic transfer. However, metal atoms intend to aggregate into clusters when their concentration is large due to their high cohesive energies compared with those of metal atoms adsorbed on graphene, which may significantly reduce the hydrogen uptake.²¹ For Al, the cohesive energy is -3.39 eV .²² To examine the validity of this assumption, a unit cell with eight C atoms and one Al atom is used in the present study, which is shown in Fig. 1. The ratio Al:C=1:8 is quite moderate and moreover strictly obeys the doping rules for high coverage metals,^{23,24} which makes it possible for us to achieve a relatively high storage capacity. This rule ensures that the Al-Al distance is sufficiently large avoiding clustering of Al on graphene.

The favorite adsorption position of this Al atom on graphene is then determined. There are three different adsorption sites as shown in Fig. 1, which are the hollow of the carbon hexagon (H), the bridge of C-C bond (B), and the top site of the C atom (T), respectively. The Al-Al interaction is indeed negligible owing to the large distance of about 4.92 \AA . It is found that the Al adsorbed at the H site has the lowest energy and is therefore the favorite adsorption configuration with a binding energy of -0.824 eV and the distance between Al and the graphene layer d_1 is about 2.079 \AA . In Fig. 1, the charges of atoms near the adsorbed Al atom are given, which are obtained by Mulliken analysis. The adsorbed Al atom has a positive $0.266e$ charge while each C atom nearby has a negative charge $-0.049e$. Note that the other two C atoms in the simulation cell contribute the rest of the electron charge to the negative C atoms. Therefore, the long distance of Al-Al, the relative strong bonding between the Al atom and the graphene layer, and the Coulomb repulsion between the Al atoms prevent metal aggregation on graphene.

Due to the positive charge on the Al atoms and the negative charge on the carbon atoms, an electric field is induced

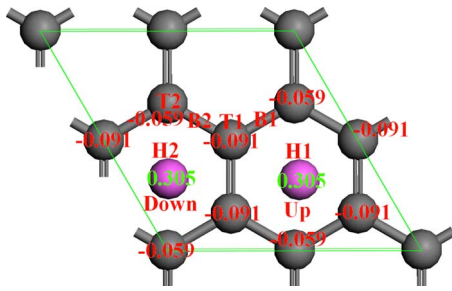


FIG. 3. (Color online) Six different adsorption sites for the second Al atom on the other side of the graphene layer. The charges of atoms near the adsorbed Al atoms are also given, where the unit of charge is one electron charge e .

between the Al atoms and the graphene layer, which in turn leads to a backtransfer of charge from the graphene layer to the Al atom. Hence, by increasing Al coverage, adsorbed Al atoms would become less positively charged, which would decrease the Coulomb repulsion between the Al atoms, and eventually this may lead to metal aggregation. This also agrees with the doping rules.^{23,24}

To further confirm the stability of Al atoms on graphene, the diffusion behavior of an Al atom on graphene was studied by the transition search (TS) method in order to obtain the diffusion barrier. We have shown above that the most stable configuration of an Al atom on graphene corresponds to adsorption on the H site of graphene. Consequently, we next consider the diffusion scenario of an Al atom on graphene between two H sites in order to study surface diffusion. Based on the TS calculation, we found that the classical barrier for surface diffusion is 0.104 eV. Notice that the calculated diffusion barrier corresponds only to a classical hopping model of diffusion. In practical cases, quantum tunneling effects should also be considered.²⁵ In addition, because only a single Al atom is involved in the simulation cell, the Al-Al distance is kept unchanged. While in actual diffusion, the Al-Al distance would be shortened and repulsive Coulomb interaction among positively charged Al atoms would increase, leading to a significant increase in the diffusion barrier, which will prevent aggregation of adsorbed Al atoms on graphene.

We consider next the adsorption of Al atoms on both sides of the graphene layer in order to increase the available surface area for hydrogen storage since the charged metal atoms are the nucleation centers for hydrogen adsorption.⁴⁻⁶ As shown in Fig. 3, there are six different sites for the second Al atom to be positioned on the other side of the graphene layer. After geometry optimization of the six configurations, we found that the lowest-energy configuration is realized for the second Al atom adsorbed on the H2 site with energy $E_{b,Al} = -1.096$ eV and the average $E_{b,Al}$ for the two Al atoms is -0.960 eV. As shown in Fig. 3, the two Al atoms are positioned on two shoulder-by-shoulder carbon hexagons but on opposite sides of the graphene layer. The repulsive Coulomb interaction between the positively charged Al atoms on the upper and lower parts of the graphene plane is screened by the negative charge on the C atoms. The graphene layer is now more negatively charged as compared to the previous single Al atom case while the adsorbed Al atoms are more

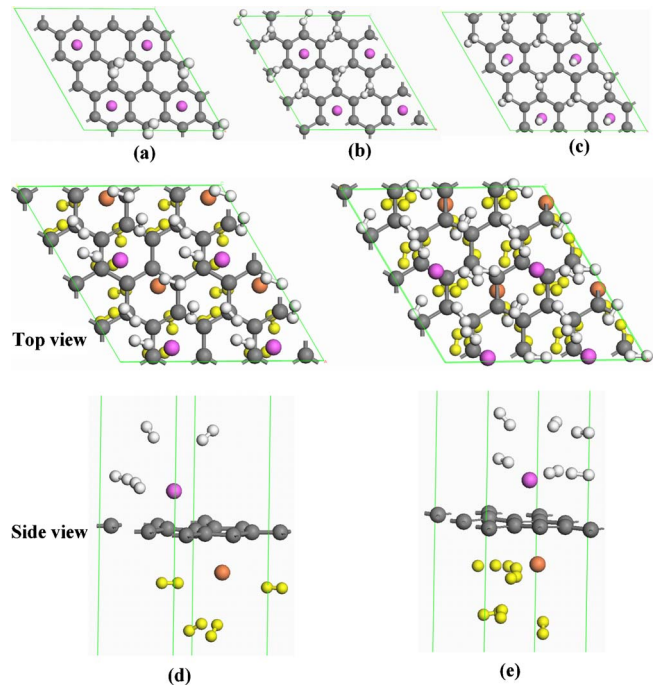


FIG. 4. (Color online) Atomic structures of H_2 molecules adsorbed on Al-adsorbed graphene. (a) One H_2 molecule adsorbed on graphene with Al adsorbed on the single side, (b) two H_2 molecules adsorbed on graphene with Al adsorbed on a single side of graphene, (c) three H_2 molecules adsorbed on graphene with Al adsorbed on one side of graphene, (d) four H_2 molecules adsorbed on each side of graphene with Al adsorbed on its both sides, and (e) six H_2 molecules adsorbed on each side of graphene with Al adsorbed on its both sides. In this figure, we plotted $4 \times 4 \times 1$ supercells to better display the adsorption sites of the H_2 molecules. In (d) and (e), due to the Al atoms and H_2 molecules adsorbed on both sides of graphene, Al atoms and H_2 molecules below the graphene layer are shown as orange and yellow, respectively. Meanwhile, in order to show the two-layer adsorption arrangement of H_2 molecules, initial simulation cells of side view are also given in the nether part of (d) and (e).

positively charged (the charges of the atoms on the Al and C atoms are given in Fig. 3). It leads to a stronger binding energy for the Al atoms on the graphene. In addition, $d_1 \approx 2.138$ Å which is slightly larger as compared to the case of single side adsorption, which is counterintuitive. The reason is that the small increase in d_1 is a result of the Coulomb repulsion between the two positively charged Al atoms located above and below the graphene layer, which is screened by the charged graphene layer.

B. Adsorption of H_2 molecules on Al-adsorbed single side graphene

For the case of one H_2 molecule adsorbed on graphene with Al atoms adsorbed on a single side of graphene, the configuration after relaxation is shown in Fig. 4(a) where a $4 \times 4 \times 1$ supercell is taken in order to better display the atomic structure, especially the adsorption site of the H_2 molecule. It indicates that the H_2 molecule would take the center site of equilateral triangles formed by adsorbed Al atoms.

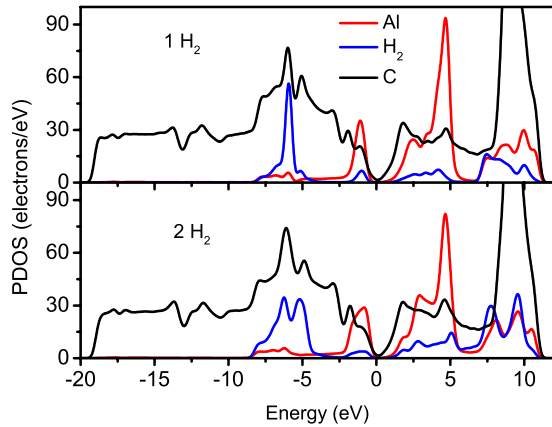


FIG. 5. (Color online) PDOS of Al, H_2 , and C in the systems of one and two H_2 molecules adsorbed on graphene with Al adsorbed on the single side. The Fermi level is at 0.

The vertical distance between the H_2 molecules and the graphene layer is $d_2 = 2.830 \text{ \AA}$, while d_1 decreases slightly to 2.060 \AA , and the adsorption energy for the first H_2 molecule is $E_{b-H_2} = -0.182 \text{ eV}/H_2$. In the figure, we see that a parallelogram formed by the adsorbed Al atoms has two center sites of equilateral triangles. However, due to the limitation of interaction among adsorbed H_2 molecules, H_2 would take just one of the two center sites. When more H_2 molecules are adsorbed, the two center sites would be both occupied as shown in Fig. 4(b) where two H_2 molecules are adsorbed. The adsorption energy for the second H_2 molecule is $E_{b-H_2} = -0.273 \text{ eV}/H_2$, which gives an average adsorption energy for the two H_2 molecules of $-0.227 \text{ eV}/H_2$. Figure 4(c) gives the atomic structure of three adsorbed H_2 molecules. Two H_2 molecules take the two center sites as in Fig. 4(b), the other H_2 molecule would take the top site of the Al atom. The distance of the three H_2 to the Al atom are, respectively, 2.786 \AA , 2.879 \AA , and 2.903 \AA with average binding energy of $-0.176 \text{ eV}/H_2$. If we further increase the number of H_2 molecules, after relaxation, the result shows that the fourth H_2 molecule cannot be adsorbed. Therefore, we conclude that the maximum number of H_2 molecules adsorbed on a single side of a $2 \times 2 \times 1$ graphene unit cell is 3.

For the cases of one and two adsorbed H_2 molecules, we found that the H_2 molecules are parallel to the graphene layer

and all H_2 molecules are equidistant from the Al atoms. Once the number of H_2 absorbed on each Al atom exceeded two, the absorbed H_2 molecules tend to tilt toward the Al atoms because of the increased positive charge of the Al atoms and the symmetry of the bonding configuration of the H_2 molecules. This phenomenon is similar to the case of adsorption of H_2 molecules on Ca-adsorbed graphene.⁵

In addition, we notice that the E_{b-H_2} of the second H_2 molecule is much larger than that of the first one, i.e., it is about 50% larger. In order to understand this enhancement, the projected density of states (PDOS) of Al, C atoms, and H_2 molecules are plotted and shown in Fig. 5. It was reported that the band broadening of the molecular level of H_2 below the Fermi energy indicates a significant H_2 - H_2 interaction that in turn increases its binding energy to the substrate.⁵ The same mechanism is found here where the band broadening of about -6 eV appears in Fig. 5. In fact, the binding energy of the first H_2 molecule to the Al atom which prefers to be parallel to the graphene layer is generally small.⁵

Figure 6 displays the electron density of the system with one and two adsorbed H_2 molecules. Notice that there is nonzero electron density in the region between the graphene layer and the adsorbed Al atom. This is the reason why Al atoms are strongly adsorbed on the graphene layer. In addition, some electronic distribution also appears among the H_2 molecules, the Al atom, and the graphene layer. For H_2 molecules adsorbed on pristine graphene, no electron density was found between the H_2 molecules and the graphene layer.¹² Therefore, H_2 adsorption is enhanced in the Al-adsorbed graphene system due to the adsorbed Al atoms that act as bridges to link the electron clouds of the H_2 molecules and the graphene layer. Furthermore, Fig. 6(b) also shows that there is some electron distribution between the two adsorbed H_2 molecules. This means that the interaction between the H_2 molecules will change the electron distribution and may induce an enhancement of the adsorption energy as found in Fig. 5.

Very recently, Cha *et al.*¹¹ investigated the mechanism of H_2 adsorption onto Ca-cation centers using both DFT and wave-function approaches. They found that DFT calculations overestimated significantly the binding energy between the H_2 molecules and the Ca^{1+} cation centers. In light of this paper, we carried out a calculation on two H_2 molecules

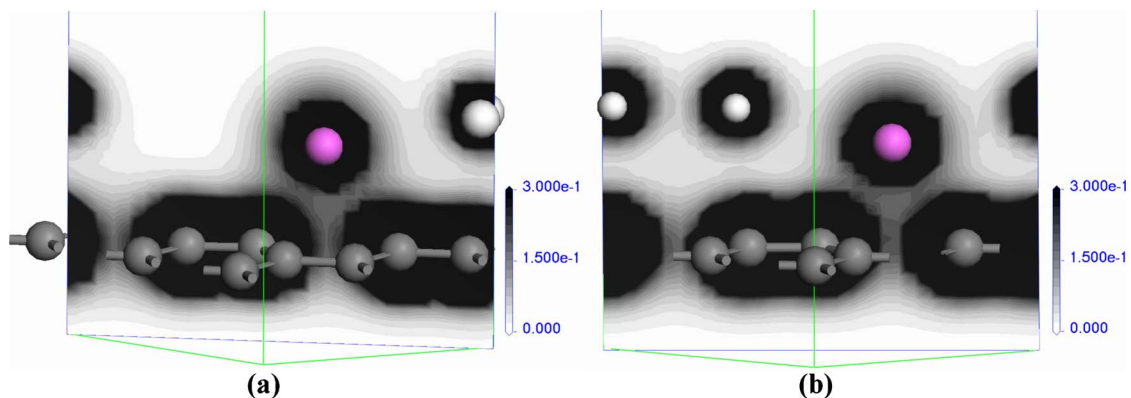


FIG. 6. (Color online) Electron-density distribution in the systems of one and two H_2 molecules adsorbed on graphene with Al adsorbed on a single side of graphene.

adsorbed on an Al-coated graphene using the cluster model with both LDA and wave-function approaches with MP2 within the Gaussian modules. The average binding energies for H_2 in this cluster system were found to be -0.196 eV/ H_2 and -0.185 eV/ H_2 with LDA and MP2, respectively. Thus the two values differ by less than 6% giving some credibility to our numerical obtained binding energy. In other words, the significant overestimation by DFT as found earlier for the binding of H_2 molecules onto Ca^{1+} system does not occur for our system.

In addition, in order to investigate the effect of the simulation cell size on the results we also performed calculations using a $4 \times 4 \times 1$ supercell with H_2 molecules adsorbed as shown in Fig. 4(a). We found almost the same results as obtained with the $2 \times 2 \times 1$ supercell. In the $4 \times 4 \times 1$ system, the H_2 molecules are adsorbed on the center sites of the equilateral triangles of Al atoms, as shown in Fig. 4(a). The distance between the H_2 molecules and the graphene surface are, respectively, 2.884 Å and 2.825 Å in $2 \times 2 \times 1$ and $4 \times 4 \times 1$ systems, while E_{b-H_2} in $4 \times 4 \times 1$ system is -0.190 eV/ H_2 and $E_{b-H_2} = -0.182$ eV/ H_2 in $2 \times 2 \times 1$ system.

C. Adsorption of H_2 molecules on Al adsorbed on both sides of graphene

For the case of hydrogen adsorption on Al that is adsorbed on both sides of graphene, the situations of one, two, and three H_2 molecules adsorbed on each side of graphene are rather similar to the above case of adsorption on a single side of graphene. In other words, two H_2 molecules will take the center sites of equilateral triangles formed by the adsorbed Al atoms as shown in Figs. 4(a) and 4(b), and the third H_2 will take the top site of the Al atom as in Fig. 4(c). Previously, we saw that a maximum of three H_2 molecules per $2 \times 2 \times 1$ unit cell can be adsorbed on one side of graphene. However, for the case of adsorption on both sides of the graphene layer, each side can adsorb more than three H_2 molecules. In Fig. 4(d) with four H_2 molecules adsorbed on each side, we show a $4 \times 4 \times 1$ supercell. Two of them take the center sites of equilateral triangles and the other two are located on the bridge sites of two Al atoms. However, the four H_2 molecules are in two different planes with distances to the graphene layer being 2.672 and 4.675 Å. The distances of the four H_2 molecules to the Al atom are, respectively, 2.444 Å, 2.531 Å, 2.918 Å, and 2.947 Å. The average E_{b-H_2} is -0.209 eV/ H_2 . If we further increase the number of H_2 molecules, the two H_2 molecules in the center sites of the equilateral triangles will hop to the bridge sites of the two Al atoms while keeping the two-layer structure. Therefore, each Al atom can adsorb a maximum of six H_2 molecules due to the two-layer adsorption structure and each Al atom has six nearest Al atoms with each adsorbed H_2 molecule shared by two Al atoms. Figure 4(e) gives the corresponding atomic structure with H_2 molecules fully adsorbed. It shows that all the H_2 molecules are located at the bridge sites of Al-Al and are arranged into two layers on each side of graphene. Note that the adsorption of H_2 on both sides of graphene will automatically change the sites of ad-

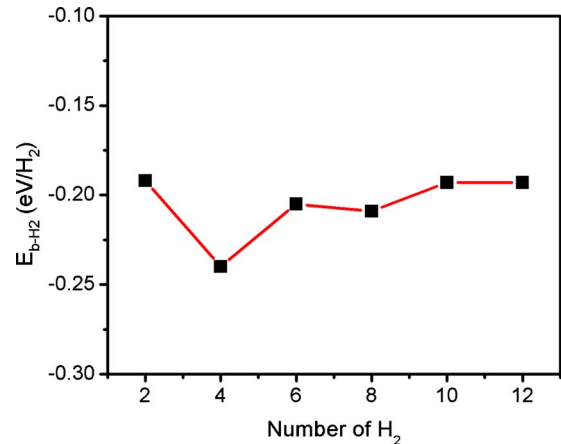


FIG. 7. (Color online) X -dependent average adsorption energy $E_{b-H_2}(X)$ of H_2 on graphene with Al adsorbed on both sides of graphene.

sorbed Al atoms from the center site of the carbon hexagon to nearly the bridge site of the C-C bond as shown in Figs. 4(d) and 4(e). The different location of the Al atoms in the presence of adsorbed H_2 for single side and both sides of graphene is a consequence of: (1) the different charges of Al atoms adsorbed on one side of graphene and on both sides of graphene, and (2) the different number of adsorbed H_2 molecules. Therefore, HSC is up to 13.79 wt % with an average $E_{b-H_2} = -0.193$ eV/ H_2 . Note that the obtained HSC is in excess of 6 wt %, surpassing DOE's target, and the obtained E_{b-H_2} is almost within the required range of -0.2 to -0.6 eV/ H_2 .²⁶ For practical purpose, E_{b-H_2} is required to be a weak function of the adsorption coverage X of H_2 molecules on graphene, so that the adsorbed H_2 molecules can be desorbed to almost zero X . In our case, E_{b-H_2} is about -0.2 eV/ H_2 and we found that the amount of coverage has only a weak effect on E_{b-H_2} . The coverage dependence of $E_{b-H_2}(X)$ is shown in Fig. 7 with $E_{b-H_2}(X)$ varying within 15%. Note that E_{b-H_2} is the lowest when four H_2 molecules were adsorbed. This is because adsorption is strongest when H_2 molecules are located on the center sites of equilateral triangles formed by the adsorbed Al atoms. This was confirmed above in Fig. 4(a) where one H_2 molecule was first adsorbed at the center sites of the equilateral triangles. Due to the interaction between the H_2 molecules as shown in Figs. 5 and 6 and discussed above, adsorption with two H_2 molecules on each side on the center sites of equilateral triangles is strongest.

When 12 H_2 molecules are adsorbed on both sides of a $2 \times 2 \times 1$ supercell of graphene, the H_2 molecules on each side of graphene will be arranged into two layers as shown in Fig. 4(e), the distances of each layer to the graphene surface are, respectively, about 2.5 Å and 5.0 Å, while d_1 is about 2.2 Å. As discussed above, the adsorption energy E_{b-Al} for adsorption on both sides of graphene is larger than that for single side adsorption. At the same time, the Al atoms are more positively charged, and the C atoms are more negatively charged when the Al atoms are adsorbed on both sides of graphene. As found previously hydrogen adsorption is mainly induced by charged metal atoms and the strength of

the adsorption depends on the amount of the transferred charge.^{6,9} Thus, the graphene layer when Al is adsorbed on both sides of graphene has a larger capacity for H₂ storage. However, due to the limited space between the Al atoms and the repulsive interaction between the adsorbed H₂ molecules, some adsorbed H₂ molecules move upwards, over the Al atoms. This is also the reason why H₂ molecules can form a two-layer arrangement in the case of Al adsorbed on both sides of graphene, only a single H₂ layer is found for the corresponding single side system.

To test the stability of the hydrogen storage system, we performed *ab initio* molecular-dynamics (MD) simulations on a 12H₂-Al-graphene system which is shown in Fig. 4(e). The MD simulation in the NVT ensemble, i.e., constant number of atoms N , volume V , and temperature T , was performed over a time of 1 ps with a massive generalized Gaussian moments (GGM) thermostat at 300 K and without external pressure. We found that only the outer two H₂ molecules are escaping from each side of the graphene layer because they are more weakly bound than the other H₂ molecules. For example, the first H₂ molecule that is released has a binding energy of -0.129 eV. In this case, the HSC becomes 9.64 wt %, which is still much higher than DOE's target. While *ab initio* MD simulation is quite computationally time consumption, 1 ps is not enough to get statistically meaningful values for the desorption temperature. However, it does suggest that the system keeps a rather high hydrogen storage capacity at room temperature. This is even the case in the absence of external pressure and it is thus possible to release H₂ molecules without removing the Al atoms. Note that the system stability of hydrogen storage in Ti-decorated carbon nanotubes was tested in similar conditions, where the MD calculations lasted 1.5 ps.²⁷ In addition, the release of H₂ molecules can be further prevented by decreasing the temperature or increasing the pressure of storage to increase its HSC.²

To investigate the effect of the concentration of adsorbed Al atoms on its hydrogen storage capacity, we considered a $4 \times 4 \times 1$ graphene supercell with one Al atom on the center site of the carbon hexagon above and below the graphene layer. We found that each Al atom can maximally adsorb six H₂ molecules with average $E_{b-H_2} = -0.172$ eV/H₂ resulting in a HSC of 5.19 wt %. The adsorption configuration is shown in Fig. 8. Note that the HSC is much lower than the 13.79 wt % we found for the $2 \times 2 \times 1$ supercell system. In the case of H₂ adsorbed in the $2 \times 2 \times 1$ system, the H₂ molecules are adsorbed on the bridge sites of Al-Al and are arranged into a two-layer configuration. Thus, each adsorbed H₂ molecule interacts with the nearest two Al atoms. In the $4 \times 4 \times 1$ system, which corresponds to a lower density of adsorbed Al, the distance between two Al atoms is very long, up to 9.84 Å. Thus, each H₂ interacts with one Al atom and the graphene layer, and there is more space available for the adsorbed H₂ molecules which are located in a single layer. The corresponding adsorption energies E_{b-H_2} also decrease slightly as the Al-Al distance increases. For single H₂ molecule and two H₂ molecules adsorbed on a $4 \times 4 \times 1$ supercell, E_{b-H_2} are -0.169 and -0.178 eV/H₂. In case of a $2 \times 2 \times 1$ supercell we found that E_{b-H_2} are -0.182 eV/H₂ and -0.227 eV/H₂, respectively.

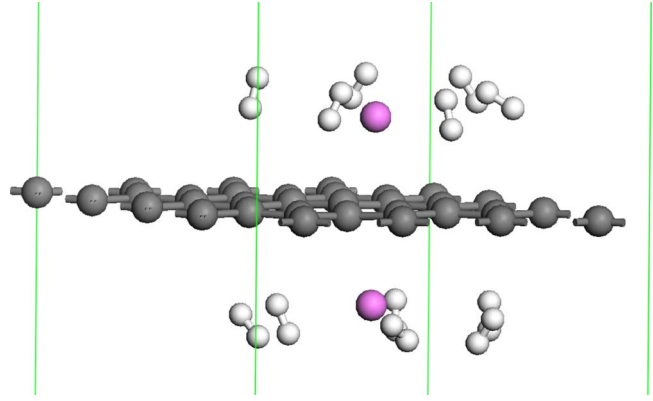


FIG. 8. (Color online) The configuration of H₂ molecules adsorbed in a $4 \times 4 \times 1$ supercell system.

For practical applications, it is desirable to know the exact charge status of the hydrogen storage material. From it we can obtain information whether the hydrogen storage material is fully charged or the adsorbed H₂ molecules are completely released. The charge exchanged with the graphene layer can be determined by the conductivity of the graphene layer, which is strongly determined by the DOS at the Fermi level.^{28,29} The X dependence of the latter quantity is given in Fig. 9. The result shows that the DOS at the Fermi level decreases as X increases and this dependence becomes weaker at high X .

IV. CONCLUSION

In conclusion, the adsorption of Al atoms on a graphene layer and of H₂ molecules on Al-adsorbed graphene was studied using density-functional theory. We found that the Al atoms are strongly adsorbed on graphene. A graphene layer with adsorbed Al atoms on both sides has an excellent hydrogen storage capacity up to 13.79 wt %, which is in excess of 6 wt %, surpassing DOE's target, where a two-layer arrangement of H₂ molecules is formed on each side of graphene. The average adsorption energy of H₂ on Al-

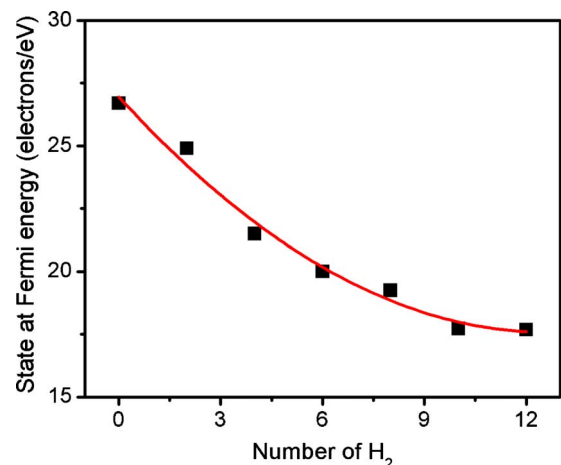


FIG. 9. (Color online) X -dependent number of band states at the Fermi level.

adsorbed graphene is -0.193 eV/H₂ which is also in a range, such that hydrogen adsorption/desorption can be recycled at near ambient conditions. After analyzing the density of states and the electron-density distribution of the adsorbed systems, we found that the hydrogen storage enhancement mechanism is due to the adsorbed Al atoms that alter the electron distribution of both the H₂ molecules and the graphene layer and bridge their electron clouds, which leads to a strengthening of the adsorption of H₂ mol-

ecules. Furthermore, the conductivity of the graphene layer depends on X , which suggests that the concentration of H₂ stored in this material can be detected by measuring its conductivity change.

ACKNOWLEDGMENTS

This work was supported by the Flemish Science Foundation (FWO) and the Belgian Science Policy (IAP).

*francois.peeters@ua.ac.be

- ¹S. A. Shevlin and Z. X. Guo, *Chem. Soc. Rev.* **38**, 211 (2009).
- ²U. Sahaym and M. G. Norton, *J. Mater. Sci.* **43**, 5395 (2008).
- ³M. Yoon, S. Yang, C. Hicke, E. Wang, and Z. Zhang, *Nano Lett.* **7**, 2578 (2007).
- ⁴M. Yoon, S. Yang, C. Hicke, E. Wang, D. Geohegan, and Z. Zhang, *Phys. Rev. Lett.* **100**, 206806 (2008).
- ⁵C. Ataca, E. Aktürk, and S. Ciraci, *Phys. Rev. B* **79**, 041406(R) (2009).
- ⁶W. Liu, Y. H. Zhao, Y. Li, Q. Jiang, and E. J. Lavernia, *J. Phys. Chem. C* **113**, 2028 (2009).
- ⁷E. Klontzas, A. Mavrandonakis, E. Tylianakis, and G. E. Froudakis, *Nano Lett.* **8**, 1572 (2008).
- ⁸W. Q. Deng, X. Xu, and W. A. Goddard, *Phys. Rev. Lett.* **92**, 166103 (2004).
- ⁹Q. Sun, P. Jena, Q. Wang, and M. Marquez, *J. Am. Chem. Soc.* **128**, 9741 (2006).
- ¹⁰E. Durgun, S. Ciraci, W. Zhou, and T. Yildirim, *Phys. Rev. Lett.* **97**, 226102 (2006).
- ¹¹J. Cha, S. Lim, C. H. Choi, M.-H. Cha, and N. Park, *Phys. Rev. Lett.* **103**, 216102 (2009).
- ¹²Z. M. Ao, Q. Jiang, R. Q. Zhang, T. T. Tan, and S. Li, *J. Appl. Phys.* **105**, 074307 (2009).
- ¹³I. Cabria, M. J. López, and J. A. Alonso, *J. Chem. Phys.* **128**, 144704 (2008).
- ¹⁴Y. Okamoto and Y. Miyamoto, *J. Phys. Chem. B* **105**, 3470 (2001).
- ¹⁵A. Lugo-Solis and I. Vasiliev, *Phys. Rev. B* **76**, 235431 (2007).
- ¹⁶O. Leenaerts, B. Partoens, and F. M. Peeters, *Phys. Rev. B* **77**, 125416 (2008).
- ¹⁷K. Tada, S. Furuya, and K. Watanabe, *Phys. Rev. B* **63**, 155405 (2001).
- ¹⁸L. A. Girifalco and M. Hodak, *Phys. Rev. B* **65**, 125404 (2002).
- ¹⁹B. Delley, *J. Chem. Phys.* **92**, 508 (1990).
- ²⁰D. R. Lide, *CRC Handbook of Chemistry and Physics*, 81st ed. (CRC Press, Boca Raton, FL, 2000).
- ²¹P. O. Krasnov, F. Ding, A. K. Singh, and B. I. Yakobson, *J. Phys. Chem. C* **111**, 17977 (2007).
- ²²R. Gaudoin, W. M. C. Foulkes, and G. Rajagopal, *J. Phys.: Condens. Matter* **14**, 8787 (2002).
- ²³G. Gao, T. Gagin, and W. A. Goddard III, *Phys. Rev. Lett.* **80**, 5556 (1998).
- ²⁴G. E. Froudakis, *Nano Lett.* **1**, 531 (2001).
- ²⁵G. Wu, J. Zhang, Y. Wu, Q. Li, K. Chou, and X. Bao, *J. Alloys Compd.* **480**, 788 (2009).
- ²⁶J. Li, T. Furuta, H. Goto, T. Ohashi, Y. Fujiwara, and S. Yip, *J. Chem. Phys.* **119**, 2376 (2003).
- ²⁷T. Yildirim and S. Ciraci, *Phys. Rev. Lett.* **94**, 175501 (2005).
- ²⁸F. Schedin, A. K. Geim, S. V. Morozov, E. W. Hill, P. Blake, M. I. Katsnelson, and S. Novoselov, *Nature Mater.* **6**, 652 (2007).
- ²⁹C. He, P. Zhang, Y. F. Zhu, and Q. Jiang, *J. Phys. Chem. C* **112**, 9045 (2008).